Phytomedicine 125 (2024) 155343

Contents lists available at ScienceDirect

Phytomedicine

journal homepage: www.elsevier.com/locate/phymed

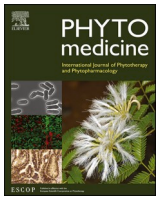

Original Article

Atranorin inhibits Zika virus infection in human glioblastoma cell line SNB-19 *via* targeting Zika virus envelope protein

Guan-gen Huang [a,b,1], Hao-yu Wang [a,c,1], Xiao-han Wang [a,c], Tao Yang [a,c], Xiao-meng Zhang [a], Chun-lan Feng [a], Wei-min Zhao [c], Wei Tang [a,b,c,*]

[a] State Key Laboratory of Chemical Biology, Shanghai Institute of Materia Medica, Chinese Academy of Sciences, Shanghai 201203, PR China
[b] School of Chinese Materia Medica, Nanjing University of Chinese Medicine, Nanjing 210023, PR China
[c] University of Chinese Academy of Sciences, Beijing 100049, PR China

ARTICLE INFO

Keywords:
Zika virus
SNB-19 cells
Atranorin
Envelope protein
Entry stage
Antiviral drugs

ABSTRACT

Background: Zika virus (ZIKV) is a single-stranded RNA flavivirus transmitted by mosquitoes. Its infection is associated with neurological complications such as neonatal microcephaly and adult Guillain–Barré syndrome, posing a serious threat to the health of people worldwide. Therefore, there is an urgent need to develop effective anti-ZIKV drugs. Atranorin is a lichen secondary metabolite with a wide range of biological activities, including anti-inflammatory, antibacterial and antioxidant, etc. However, the antiviral activity of atranorin and underlying mechanism has not been fully elucidated.

Purpose: We aimed to determine the anti-ZIKV activity of atranorin in human glioma cell line SNB-19 and investigate the potential mechanism from the perspective of viral life cycle and the host cell functions.

Methods: We first established ZIKV-infected human glioma cells (SNB-19) model and used Western Blot, RT-qPCR, immunofluorescence, fluorescence-activated cell sorting (FACS) and plaque assay to evaluate the anti-ZIKV activity of atranorin. Then we assessed the regulation effect of atranorin on ZIKV induced IFN signal pathway activation by RT-qPCR. Afterward, we introduced time-of-addition assay, viral adsorption assay, viral internalization assay and transferrin uptake assay to define which step of ZIKV lifecycle is influenced by atranorin. Finally, we performed virus infectivity assay, molecular docking and thermal shift assay to uncover the target protein of atranorin on ZIKV.

Results: Our study showed that atranorin could protect SNB-19 cells from ZIKV infection, as evidenced by inhibited viral protein expression and progeny virus yield. Meanwhile, atranorin attenuated the activation of IFN signal pathway and downstream inflammatory response that induced by ZIKV infection. The results of time-of-addition assay indicated that atranorin acted primarily by disturbing the viral entry process. After ruling out the effect of atranorin on AXL receptor tyrosine kinase (AXL) dependent virus adsorption and clathrin-mediated endocytosis, we confirmed that atranorin directly targeted the viral envelope protein and lowered ZIKV infectivity by thermal shift assay and virus infectivity assay respectively.

Conclusion: We found atranorin inhibits ZIKV infection in SNB-19 cells *via* targeting ZIKV envelope protein. Our study provided an experimental basis for the further development of atranorin and a reference for antiviral drug discovery from natural resources.

Abbreviations: AXL, AXL receptor tyrosine kinase; CPE, cell cytopathic effects; DENV, dengue virus; E protein, envelope protein; FACS, fluorescence-activated cell sorting; HCV, hepatitis C virus; IFN, Interferon; ISGs, interferon stimulated genes; JEV, Japanese encephalitis virus; MOI, multiplicity of infection; MX-1, MX dynamin like GTPase 1; NOS2, nitric oxide synthase 2; OAS1, 2′-5′-oligoadenylate synthetase 1; PFU, plaque forming units; STAT1, signal transducer and activator of transcription 1; YEF, yellow fever virus; ZIKV, Zika virus.

* Corresponding author at: State Key Laboratory of Chemical Biology, Shanghai Institute of Materia Medica, Chinese Academy of Sciences, Shanghai 201203, PR China.
E-mail address: tangwei@simm.ac.cn (W. Tang).

[1] Guan-gen Huang and Hao-yu Wang contribute equally to this work.

https://doi.org/10.1016/j.phymed.2024.155343
Received 4 September 2023; Received in revised form 26 December 2023; Accepted 7 January 2024
Available online 8 January 2024

Introduction

ZIKV, an arbovirus transmitted through Aedes mosquitoes, belongs to the Flavivirus genus of Flaviviridae family, which includes dengue virus (DENV), Japanese encephalitis virus (JEV) and yellow fever virus (YEF) (Ferraris et al., 2019). ZIKV infection is associated with neurological complications such as neonatal microcephaly and adult Guillain–Barré syndrome, posing a serious threat to the health of people worldwide (Giraldo et al., 2023). ZIKV disease was declared a global public health emergency by WHO in February 2016 (Song et al., 2017). However, there is no approved vaccine or drug for ZIKV prevention or treatment.

The ZIKV genome composes an 11 kb positive single-stranded RNA that encodes three structural proteins (capsid, pre-membrane, and envelope) and seven nonstructural proteins (NS1, NS2A, NS2B, NS3, NS4A, NS4B and NS5) (Barrows et al., 2018; Hu and Sun, 2019). Structural proteins are involved in ZIKV entry, assembly and particles release, and non-structural proteins play an important role in viral polyprotein cleavage, viral replication and immune escape responses (Lin et al., 2018).

The entry stage of ZIKV infection can be divided into adsorption and subsequent internalization, which is predominantly mediated by ZIKV envelope protein (E protein) (Rey et al., 2017). First, ZIKV E protein is adsorbed to cell surface through recognizing viral entry receptors, of which AXL is the key receptor (Agrelli et al., 2019). Then, ZIKV internalizes host cells *via* clathrin mediated endocytosis. Finally, the virus membrane fuses with the endosome, releases its genome and begins to replicate (Owczarek et al., 2019). Considering the important role of E protein in virus infection, inhibitors that target the E protein are expected to have potential antiviral effects. Actually, multiple small molecules that inhibit flavivirus entry by interference with E protein have been developed (Clark et al., 2016; Kampmann et al., 2009; Pitts et al., 2019).

The Interferon (IFN) pathway is an important part of host innate immune system for defending ZIKV infection (Yuan et al., 2021). The IFNs produced by infected cells bind to their cognate receptor and trigger the phosphorylation of the transcription factor STAT-1, leading to the expression of interferon stimulated genes (ISGs) and antiviral effects (Schneider et al., 2014). Activation of signal transducer and activator of transcription 1 (STAT1) promotes the transcription of key immune effectors such as CXCL10, CCL5 and nitric oxide synthase 2 (NOS2), resulting in recruitment, infiltration and activation of immune cells (Rauch et al., 2013). Therefore, regulation of IFN/STAT1 pathway is applicable for controlling ZIKV infection (Tolomeo et al., 2022).

Lichens are the symbiotic plants that comprise a fungus and one or more autotrophic photosynthetic species (algae or cyanobacteria). They could be achieved easily because they can grow in diverse and strict conditions, either at polar latitudes, or at extreme altitudes (Suzuki et al., 2016). The depside atranorin (C19H18O8) is one of the most common lichen secondary metabolites. Notably, atranorin displays antiviral activity against hepatitis C virus (HCV) in human liver cancer cell Huh7. Also, the mechanistic study has proved the anti-HCV activity of atranorin was attributed to interfering viral entry, but not to replication (Vu et al., 2015). Similar to HCV, ZIKV is also a member of the flavivirus family. These existing results inspire us that atranorin might have potential anti-ZIKV activity.

In this study, we would first study the action of atranorin on ZIKV infection in SNB-19 cells and attempt to uncover the potential mechanism from the perspective of type I IFN pathway and viral life cycle. Our work provides not only experimental basis of atranorin against ZIKV infection but also a common reference for antiviral drug discovery from natural product.Materials and Methods

Source of atranorin and purity

Atranorin was kindly provided by Prof. Wei-min Zhao at SIMM. The purity of atranorin was above 97% as indicated by the HPLC profile (Fig. S1A). The structure of atranorin was validated by 1H NMR spectra (Fig. S1B)

Cells and virus

Vero cells (ATCC, Manassas, VA, USA), SNB-19 cells (ATCC) and HEK293T cells (ATCC) were cultured in DMEM medium (Gibco, Grand Island, NY, USA) (37 °C, 5% CO_2) containing 10% FBS (Hyclone, South Logan, UT, USA), 100 μg/ml streptomycin and 100 U/ml penicillin. ZIKV strain SZ01/2016 (GenBank number: KU866423) was a gift from Wuhan Institute of Virology.

ZIKV propagation method was described in our previous work (Xu et al., 2022). Briefly, Vero cells were infected with ZIKV and the culture supernatants containing ZIKV were harvested when significant cell cytopathic effects (CPE) appear. Then the supernatants were centrifuged, filtered through 0.45 μM membranes, aliquoted and stored at −80 °C. The ZIKV stock titers were determined by plaque assay.

CCK8 assay

For the cytotoxicity of atranorin in SNB-19 cells, cell viability was measured by the CCK8 reagent (Dojindo, Kumamoto, Japan). Briefly, SNB-19 cells in 96-well plates were incubated with different concentrations of atranorin (50 or 25 or 12.5 μM) for 48 h, followed by incubating with 20 μl CCK8 for 1 h. The OD values were measured with microplate reader (Molecular devices, San Jose, CA, USA) and the cell survival rate was calculated. The 50 % cytotoxicity concentration (CC_{50}) were determined by GraphPad Prism software 8.0 (La Jolla, CA, USA).

For the antiviral activity, SNB-19 cells in 96-well plates were incubated with different concentrations of atranorin and ZIKV (multiplicity of infection (MOI) = 2) for 48 h. The antiviral activity was determined by comparing the survival rate of ZIKV infected cells and atranorin treated cells. The 50% effective concentration (EC_{50}) values were calculated by GraphPad Prism software 8.0.

RT-qPCR assay

Total RNA was extracted with Trizol reagent (Tiangen, Beijing, China). Reverse transcription was carried out with a Trans-Script First-Strand cDNA Synthesis SuperMix Kit (YEASEN, shanghai, China) according to the manufacturer's instructions. Real-time PCR was performed on reverse transcription products with specific primers and Hifair™ qPCR SYBR Green Master Mix (YEASEN). The primers sequences were listed in Supplementary Table S1.

Western blot assay

Harvested cells were lysed with SDS buffer (Beyotime, Shanghai, China) supplemented with proteinase inhibitor (Beyotime). Electrophoresis was performed as described previously (Wang et al., 2023). Briefly, equal protein amounts were loaded to 10% SDS-PAGE and transferred to a nitrocellulose membrane (Bio-Rad, Hercules, CA, USA), which was blocked with Super-Block T20 blocking buffer (Thermo--Fisher, Waltham, MA, USA) and then incubated overnight at 4 °C with primary antibodies. The bands were incubated with HRP-conjugated anti-rabbit IgG (Bio-Rad) and further visualized using a Super-Signal West Femto Maximum Sensitivity Substrate kit (Thermo-Fisher) under a ChemiDoc MP Imaging System (Bio-Rad). The antibodies used in this study were listed in Supplementary Table S2.

Immunofluorescence assay

For the detection of ZIKV envelope protein expression levels, SNB-19 cells were incubated with atranorin and ZIKV (MOI = 2) for 48 h and then fixed with Immunol Staining Fix Solution containing paraformaldehyde (Beyotime) for 15 min at room temperature. After blocking for 1 h with the blocking buffer (Beyotime), SNB-19 cells were incubated with anti-flavivirus envelope (4G2) at 4 °C overnight, followed by multiple PBST (PBS plus Tween-20) washing and incubation

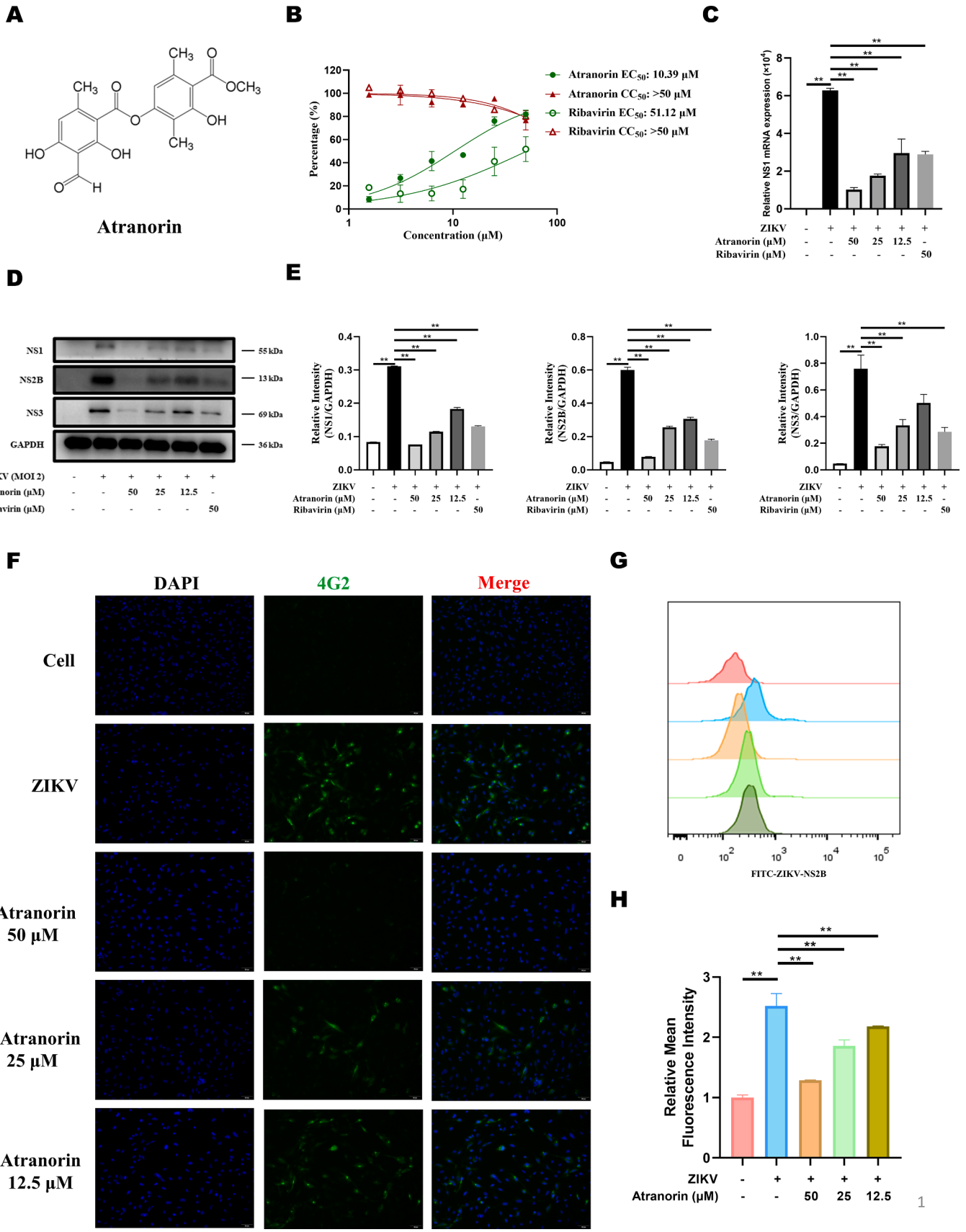

Fig. 1. Atranorin inhibited ZIKV infection in SNB-19 cells. A. The cytotoxicity and anti-ZIKV activity of atranorin in SNB-19 cells. B. The intracellular ZIKV NS1 mRNA level. C. The intracellular viral NS1, NS2B and NS3 protein level. D. The quantification of NS1, NS2B and NS3 protein level. E. ZIKV 4G2 expression and location in SNB-19 cells. Scale bar, 50 μm. F. The quantification of ZIKV NS2B fluorescence intensity. G. The quantification of relative mean fluorescence intensity of ZIKV NS2B protein. The experiments were repeated for three times. Data are shown as means ± SEM. $^{**}p < 0.01$ compared with ZIKV infection group.

with FITC-conjugated anti-rabbit secondary antibodies (Proteintech, Rocky Hill, NJ, USA) for 1 h at room temperature. Slides were mounted using Fluoroshield Mounting Medium with DAPI (Abcam, Cambridge, MA, USA). Images were captured by Olympus, IX73 (Tokyo, Japan).

Flow cytometry assay

ZIKV infected SNB-19 cells were harvested and fixed for 30 min at 4 °C followed by treatment with permeabilization buffer (eBioscience, San Diego, CA, USA). Cells were incubated with anti-ZIKV-NS2B (GeneTex, Alton Pkwy, Irvine, CA, USA) at 4 °C for 40 min and then labeled with FITC Goat anti-Rabbit IgG (H + L) secondary antibody (Proteintech) for 30 min. The ZIKV-NS2B level in SNB-19 cells were detected with LSRFortessa (BD, San Jose, CA, USA) and data were analyzed with FlowJo V10 Software.

Plaque assay

Briefly, virus was titrated onto a monolayer culture of Vero cells in 12-well plates and incubated at 37 °C for 2 h. Then the cells were washed twice with PBS to remove virus inoculum and the medium was replaced with DMEM containing 2% FBS and 1% low-melting agarose. Vero cells were incubated for an additional 4 days before fixation and incubated with crystal violet. Fixed cells were washed with flowing water and the plate was photographed for analyzing the plates for plaque forming units per ml (plaque forming units (PFU) /ml).

Time-of-addition assay

SNB-19 cells were seeded in 6 or 12-wells plate overnight. Pretreatment: cells were treated with atranorin (50 μM) for 1 h, followed by ZIKV infection for 2 h after removing atranorin by PBS washing. Then the washed cells were cultured for another 24 or 48 h. Co-treatment: cells were infected with ZIKV and treated with atranorin for 2 h, washed with PBS and cultured for 24 or 48 h. Post-treatment: cells were infected with ZIKV for 2 h, washed with PBS, then treated with atranorin and incubated for 24 or 48 h.

siRNA transfection assay

To knock down the AXL expression in SNB-19 cells, siRNA was transfected with Lipofectamine® RNAi-MAX reagent (Thermo-Fisher) according to our previous study (Xu et al., 2022). Cells were collected 24 h after transfection and AXL expression was detected by Western blot. The siRNA oligo sequences is GTGGGAGATTGCCACAAGA.

Viral adsorption assay

Vero cells were incubated with ZIKV (MOI = 2) and 50 μM atranorin for 1 h at 4 °C for the virus attaching to the cell surface. Then the cells were washed with cold PBS to remove the unattached virus and incubated at 37 °C for 1 h to permit virus entering the cells. The intracellular virus titrate was measured with plaque assay immediately.

Viral internalization assay

Vero cells were incubated with ZIKV (MOI = 2) at 4 °C for 1 h. Then the cells were washed with cold PBS and then incubated with atranorin (50 μM) at 37 °C for 1 h to allow for virus internalization. After removing the inoculum, the cells were washed with citric acid buffer (PH = 3.0) for 1 min to inactivate the extracellular virions. The intracellular virus titrate was measured with plaque assay immediately.

Transferrin uptake assay

Transferrin uptake assay was performed to observe clathrin-mediated endocytosis in HEK293T cells (Irie and Tavassoli, 1987). HEK293T cells were seeded on coverslips in 6-well plates overnight. Then the cells were pretreated with atranorin (50 μM) for 30 min and stained with 25 μg/ml AlexaFluor488-labelled human transferrin for 15 min. After that, cells were washed with acid wash buffer to remove the untaken transferrin. Finally, cells were fixed and stained with DAPI for images capturing on Olympus, IX73.

Virus infectivity assay

ZIKV was pre-incubated with atranorin (50 μM) for 1 h at 37 °C before infection. Then plaque assay was performed with the Vero cells to evaluate the infectious ability of ZIKV.

Molecular docking

The structure of E protein (PDB code 5JHM) was obtained from RCSB Protein Data Bank. The water molecules were removed in Autodock. Moreover, the center of combined area was $x = 18.458$, $y = -34.401$, $z = 25.13$, spacing 1.000 (size $x = 126.0$; $y = 100.0$; $z = 86.0$). Using hydrogens and charges tool in edit, the receptor was prepared for docking. Ligands were sketched in ChemBioDraw program and uploaded to Autodock. Furthermore, ligands were obtained through "hydrogens". The molecular docking module (Autodock Vina) was used for docking, and the simulation with the highest affinity energy which showed hydrogen bond interaction with the active site was analyzed and visualized in Pymol and Discovery Studio Visualizer.

Thermal shift assay

The temperature-dependent thermal shift assay was performed as previously described (Tan et al., 2021). Lysates from envelope-overexpressing E. coli (GENEWIZ, Jiangsu, China) were incubated with 50 μM of atranorin for 2 h at 37 °C. Control lysates were incubated with an equal volume of DMSO. Following incubation, lysates were equally divided into 7 parts, which were heated at 37, 41, 45, 49, 53, 57 and 61 °C for 3 min, respectively. Finally, each sample was added 5 × SDS loading buffer for further Western blot assay. Envelope protein expression levels was quantitatively analyzed by ImageJ and plotted with GraphPad Prism software 8.0.

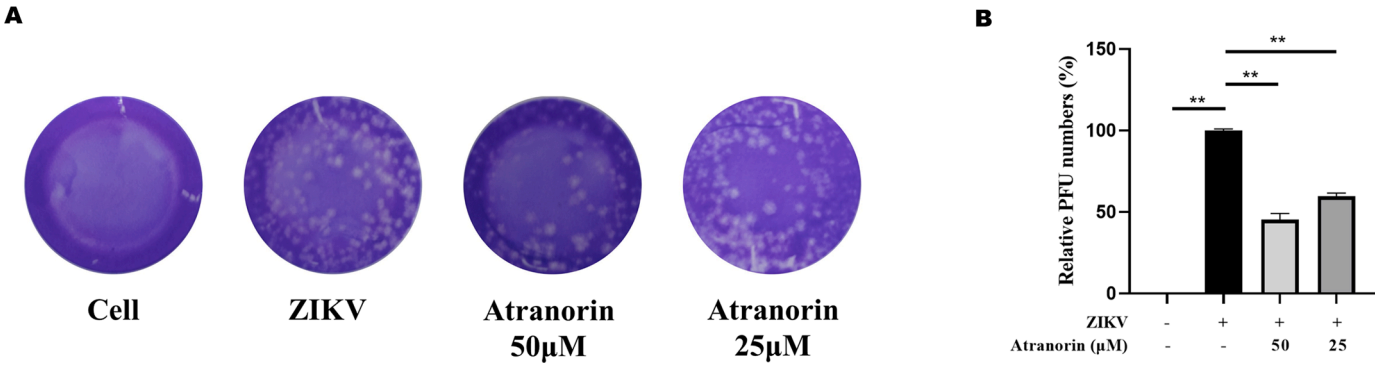

Fig. 2. Atranorin reduced progeny virus yields in ZIKV-infected SNB-19 cells. A. The progeny virus yields in SNB-19 cells culture supernatants. B. The quantification of relative PFU numbers. The experiments were repeated for three times. Data are shown as means ± SEM. $^{**}p < 0.01$ compared with ZIKV infection group.

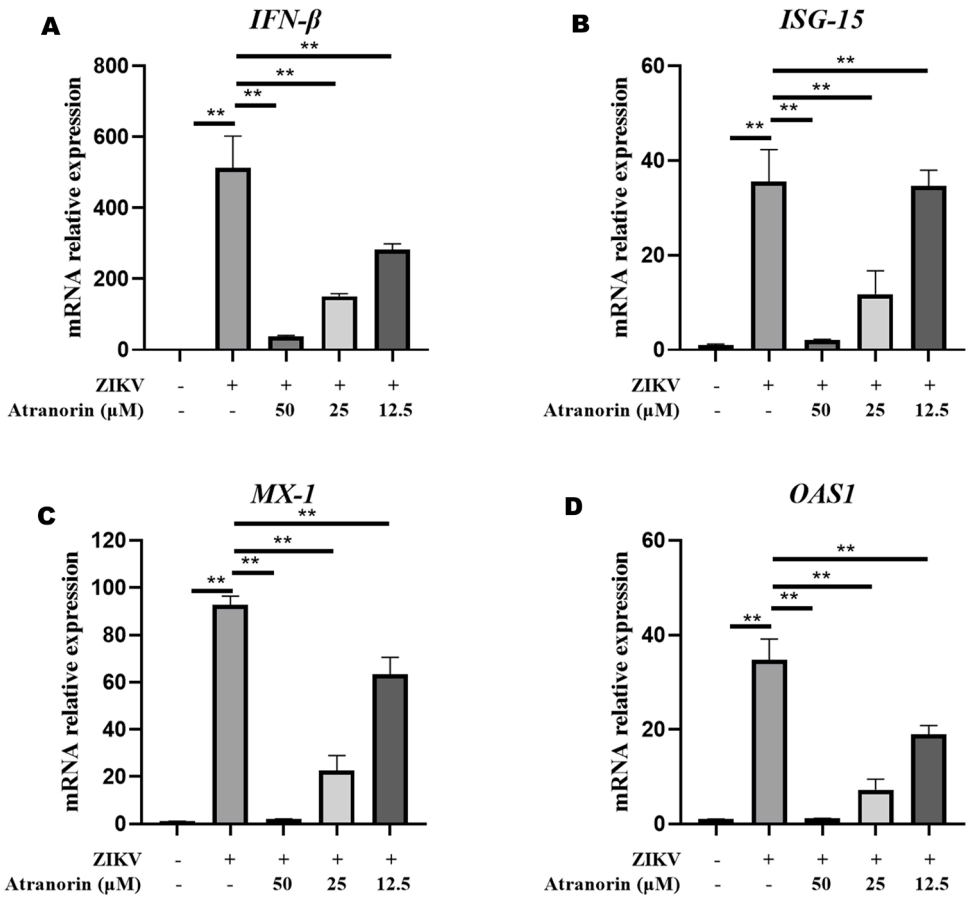

Fig. 3. Atranorin altered IFN-I-mediated antiviral responses in SNB-19 cells. A–D. The mRNA levels of IFN-β (A), ISG-15 (B), MX-1 (C) and OAS1 (D) in SNB-19 cells. The experiments were repeated for three times. Data are shown as mean ± SEM. $^{**}p < 0.01$ compared with ZIKV infection group.

Statistical analysis

All experiments were repeated at least three times and data were presented as mean ± SEM. Statistical differences were analyzed by GraphPad Prism 8.0 software using one-way analysis of variance (ANOVA). $p < 0.05$ was considered statistically significant, with increasing levels of confidence displayed as $^{*}p < 0.05$; $^{**}p < 0.01$.

Results

Atranorin inhibited ZIKV infection in SNB-19 cells

Considering the injuries effect of ZIKV on neurons (Ihunwo et al., 2022), we first examined the cytotoxicity and possible protective effect of atranorin (Fig. 1A) on human neural cell line SNB-19 by CCK8 assay. Atranorin showed little toxicity and could protect SNB-19 cells from cytopathic effects with EC_{50} of 11.90 μM (Fig. 1B). Also, atranorin treatment caused a convincing dose-dependent reduction of intracellular ZIKV NS1 gene levels (Fig. 1C) and protein expression levels (NS1, NS2B and NS3 proteins) (Fig. 1D and E). These effects were better than the broad-spectrum anti-viral drug ribavirin. Similarly, immunofluorescence assay (Fig. 1F) and flow cytometry analysis (Fig. 1G and H) confirmed that atranorin treatment inhibited ZIKV envelope protein (4G2) and NS2B protein expression. All the above results indicated the anti-ZIKV activity of atranorin in SNB-19 cells.

To further evaluate the anti-ZIKV activity of atranorin, we performed a plaque assay to determine the progeny virus yields in ZIKV-infected SNB-19 cells. Supernatants from ZIKV-infected SNB-19 cells were collected and plaque assay was subsequently performed in Vero cells. We found that atranorin-treated SNB-19 cells produced lower progeny virus, presented by reduced plaque formation in Vero cells (Fig. 2A and B). These results again confirmed that atranorin inhibited ZIKV infection in SNB-19 cells.

Atranorin altered ZIKV triggered immune response in SNB-19 cells

Viral infection activates host innate immune system, in which IFN responses are important not only in clearing intracellular virus but also for generating efficient adaptive immune responses towards infection. We found atranorin attenuated ZIKV induced IFN-β transcription, together with downstream interferon-stimulated response genes such as ISG15, MX dynamin like GTPase 1 (MX-1) and 2′−5′-oligoadenylate synthetase 1 (OAS1) (Fig. 3A–D), suggesting that atranorin altered IFN signal pathway in SNB-19 cells. STAT1 is a critical transcription factor for transducing the IFN response and subsequent inflammatory responses. Atranorin also inhibited ZIKV infection induced STAT1 phosphorylation (Fig. 4A) and the mRNA level of downstream transcription factor Irf1 (Fig. 4B) in SNB-19 cells. Meanwhile, atranorin suppressed the transcription of chemokines like CCL5 and CXCL10 (Fig. 4C and D), and pro-inflammatory cytokines like TNF-α and IL-6 (Fig. 4E and F), which are downstream effector molecules of STAT1/IRF1 pathway. Together combined, atranorin altered interferon signal pathway and antiviral gene expression during ZIKV infection. We suppose this might be related with the lowered virus titers or the anti-inflammation activity of atranorin.

Atranorin acted on the entry stage of ZIKV infection

To explore how atranorin inhibits ZIKV infection, time-of-addition assay was performed according to the schematic shown in Fig. 5A.

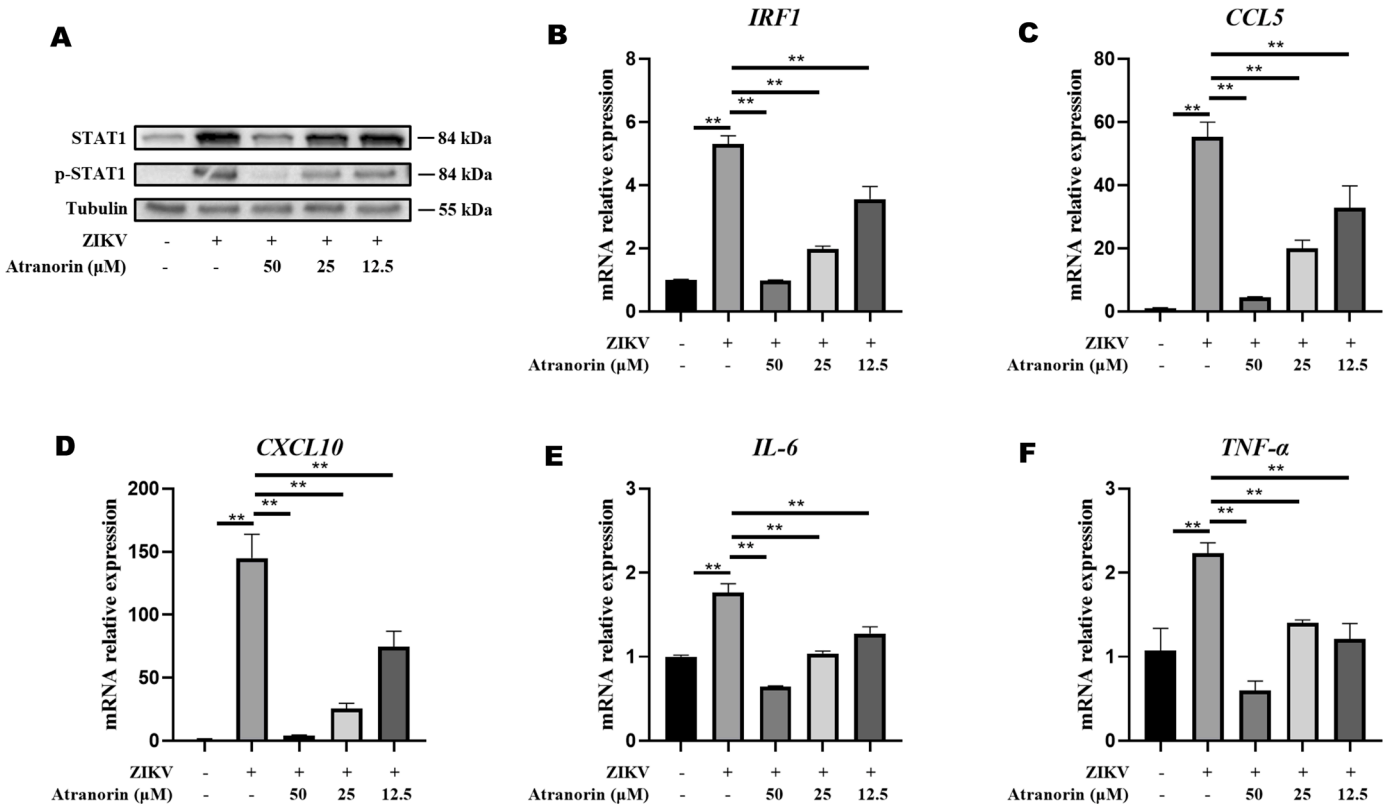

Fig. 4. Atranorin restrained ZIKV infection induced inflammatory response in SNB-19 cells. A. The protein levels of STAT1, p-STAT1 in SNB-19 cells. B–F. The mRNA levels of IRF1, CCL5, CXCL10, TNF-α and IL-6 in SNB-19 cells. The experiments were repeated for three times. Data are shown as mean ± SEM. $^{**}p < 0.01$ compared with ZIKV infection group.

When SNB-19 cells were infected with ZIKV and simultaneously treated with atranorin (co-treatment), ZIKV NS1 mRNA expression levels and protein expression levels were significantly decreased (Fig. 5B and C). Correspondingly, the percentage of ZIKV NS2B positive cell was decreased (Fig. 5D and E). Moreover, the plaque assay also showed that atranorin inhibited progeny virus production (Fig. 5F and G). However, when atranorin was incubated with SNB-19 cells before (pre-treatment) or after (post-treatment) ZIKV infection, the protective activity was weakened or even disappeared (Fig. 5B–G). Taken together, these results suggested that atranorin exerted anti-ZIKV activity mainly at the entry stage of virus infection.

Atranorin blocked ZIKV internalization without affecting adsorption

The entry stage of ZIKV infection comprises adsorption and internalization (Laureti et al., 2018). We further determined whether atranorin interferes with viral adsorption or internalization. According to the results of viral adsorption assay, atranorin failed to inhibit plaque formation, suggesting that atranorin did not influence viral adsorption (Fig. 6A and B). In addition, we found atranorin exerted anti-ZIKV activity independent of AXL (Supplementary Fig. S2A and B), which is a major receptor that mediates ZIKV envelope protein adsorption (Agrelli et al., 2019). Then we performed viral internalization assay according to the scheme shown in Fig. 6C. We found that treatment with atranorin during virus internalization significantly reduced plaque formation (Fig. 6E and F). Furthermore, we investigated whether atranorin is able to inhibit clathrin-mediated endocytosis, which is the first step of viral internalization. Similar to ZIKV, the uptake of transferrin, a typical endogenous substance, also depends on clathrin-mediated endocytosis. We found atranorin did not inhibit transferrin uptake, suggesting that atranorin did not influence clathrin-mediated endocytosis (Supplementary Fig. S3). Taken together, these data suggest that atranorin blocked ZIKV internalization without affecting adsorption.

Atranorin exerted anti-ZIKV activity by targeting viral envelope protein

After ruling out the influence of atranorin on clathrin-mediated endocytosis, we suppose atranorin might directly interact with the virus. To test our hypothesis, the virus infectivity assay was performed to compare the virus infectivity between “co-treatment” group and “pre-treatment” group during ZIKV infection process (Fig. 7A). Compared with ZIKV-atranorin co-treatment, atranorin pre-treated ZIKV showed decreased infectivity with fewer plaque formation, suggesting that atranorin might directly interact with the virus (Fig. 7B). Considering the critical role of ZIKV envelope protein in mediating virus entry, the possible direct effect of atranorin on ZIKV envelope protein becomes the major concern. We then conducted silico molecular docking assay to analyze the possible interaction between atranorin and ZIKV envelope protein. The docking results showed the optimal conformation of atranorin molecule and E protein locates between domains I and III (Fig. 7C and D). We further performed thermal shift assay to confirm the direct interaction between atranorin and ZIKV envelope protein. Pre-incubation of atranorin with envelope-overexpressing E.coli lysates increased the thermostability of E protein and retarded the heat-degradation effect on envelope (Fig. 7E and F). Therefore, these results provided direct evidence that atranorin exerted anti-ZIKV activity by targeting viral envelope protein.

Discussion

ZIKV infection is associated with neurological complications and neonatal neurological defects. However, there is no clinically approved drug or vaccine for ZIKV treatment or prevention. Although cases of Zika virus disease declined from 2017 onwards globally, transmission persists

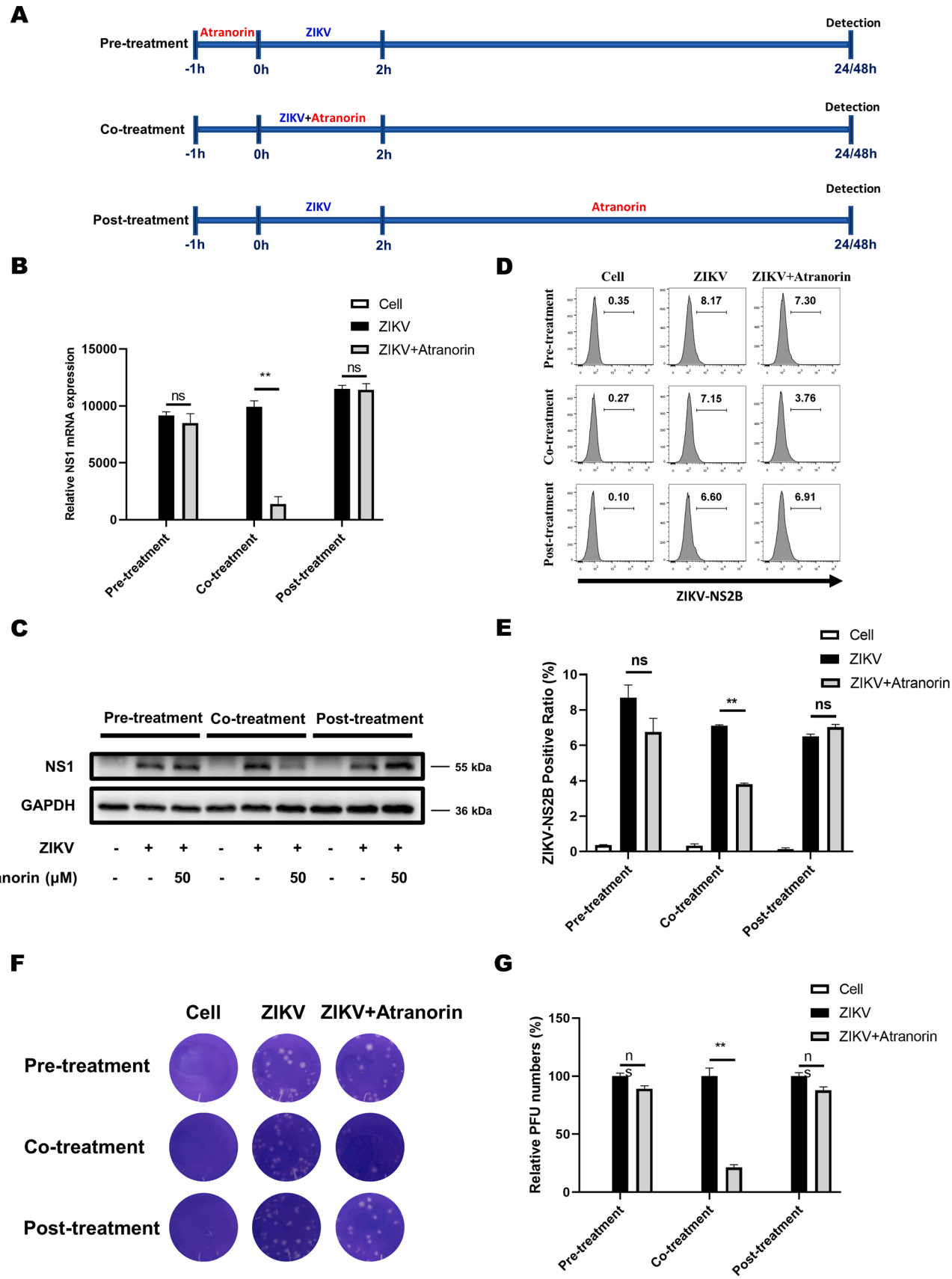

Fig. 5. Atranorin exerted anti-ZIKV activity at the entry stages. A. Schematic diagram of time-of-addition assay. B. The intracellular viral NS1 mRNA and C. The intracellular viral protein level. D. ZIKV NS2B positive cell (%). E. quantification of ZIKV NS2B protein positive cell. F. Progeny virus yield in SNB-19 cells culture supernatants. G. The quantification of relative PFU numbers. The experiments were repeated for three times. Data are shown as mean ± SEM. $^{**}p < 0.01$ compared with ZIKV infection group.

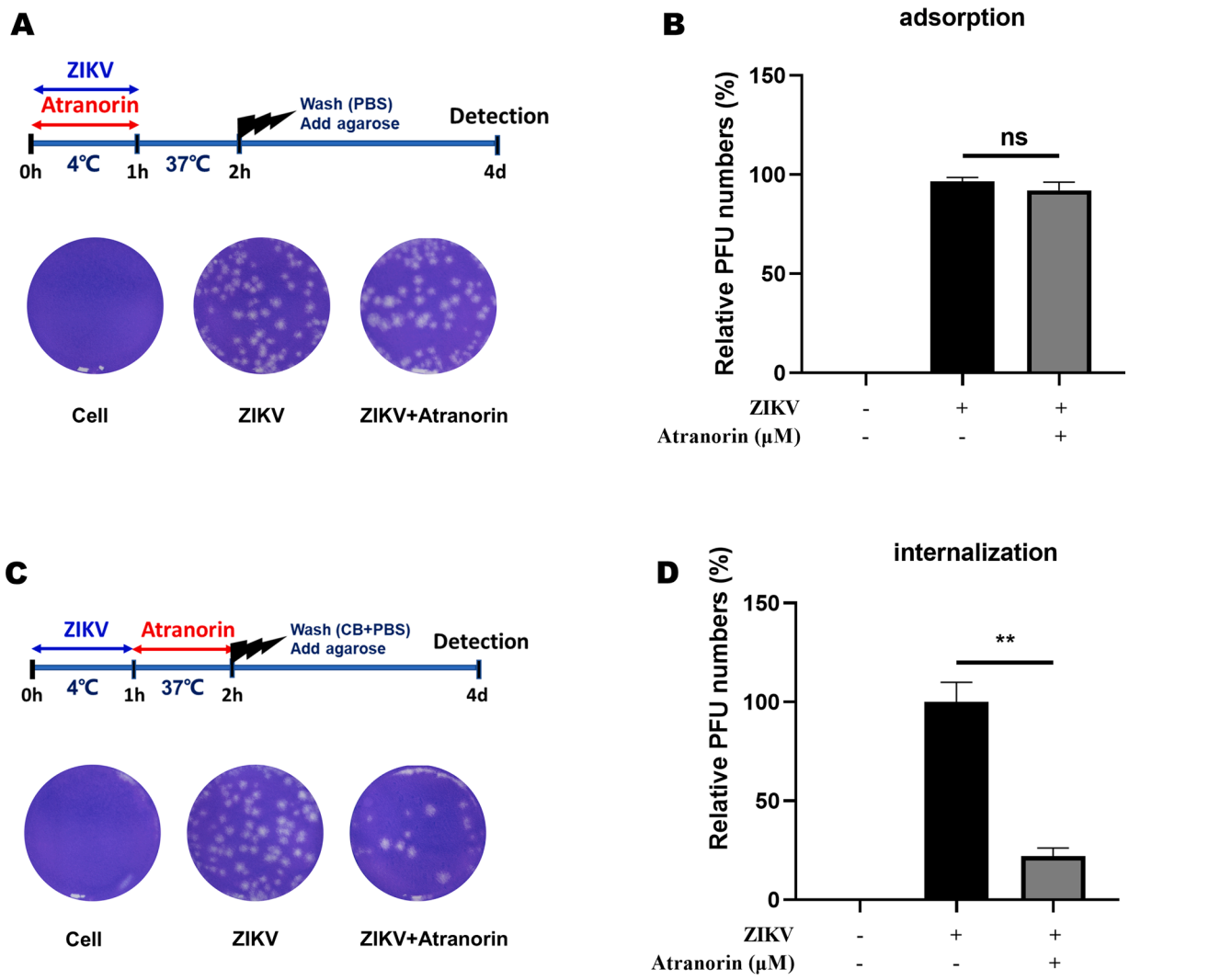

Fig. 6. Atranorin blocked ZIKV internalization without affecting adsorption. A. Schematic diagram and result of viral adsorption assay. B. The quantification of relative PFU numbers C. Schematic and result viral internalization assay. D. The quantification of relative PFU numbers. The experiments were repeated for three times. Data are shown as mean ± SEM. $^{**}p < 0.01$ compared with ZIKV infection group.

at low levels in several countries in the Americas and other endemic regions. Therefore, there is an urgent need to develop therapeutic drugs and vaccines against ZIKV.

Natural products have remarkable prospects for the application of antiviral therapy due to their broad pharmacological activities, abundant sources and low prices (Yu et al., 2018). Atranorin is a secondary metabolite of lichens. whose biological activities have been broadly studied (Studzinska-Sroka et al., 2017). Notably, the anti-HCV activity of atranorin was reported in 2015. Researchers also clarified that atranorin inhibits the entry of HCV without influencing the HCV replication (Vu et al., 2015). Nonetheless, the effect of atranorin on ZIKV, which is also a member of the flavivirus family, remains unclear. In consideration of the anti-inflammation and anti-HCV activity of atranorin, our study aims to evaluate the anti-ZIKV activity of atranorin and further investigate the potential pharmacological mechanism from the perspective of host immune-related pathways and the viral life cycle.

IFN signal pathway is an important part of the innate immune response, which is the host's first line of defending against viral invasion. The activation of IFN signal pathway induces the transcription of downstream genes such as Mx-1 and Isg to participate in the antiviral response. However, uncontrolled activation of IFN pathway in turn would arouse inflammation and host cell damage (Stephenson et al., 2018). In a cell culture model of ZIKV-infected SNB-19, we found that ZIKV infection enhance the IFN response, activate the signal transduction factor STAT1, drive the antiviral factors (ISG-15, MX-1 and OAS1) expression and induce the transcription of downstream inflammatory factors. However, atranorin intervention inhibited ZIKV induced IFN signal pathway activation and innate immune responses in SNB-19 cells. We suppose that the diminished immune response might be related to the anti-inflammation activity of atranorin (Wang et al., 2023) or the reduced intracellular ZIKV level.

To further explore which step of ZIKV lifecycle is influenced by atranorin, a time-of-addition assay was performed. Our results indicated that atranorin primarily interferes with the entry process of the ZIKV life cycle rather than influencing host factors. We then divided the entry process into viral adsorption and internalization by using adsorption assays and internalization assays. The results demonstrated that atranorin acts on the viral internalization phase, rather than adsorption. However, atranorin did not influence clathrin-mediated endocytosis, which is the key step of viral internalization. We therefore wondering whether atranorin might interact with the virus to lower its infectivity. The result of virus infectivity assay showed that pre-incubation of atranorin with virus particles could inhibit ZIKV infectivity.

The ZIKV E protein is a key protein that mediates the binding of the virus to the host receptor and the fusion of the endosome during the virus entry process. Considering the importance of ZIKV envelope

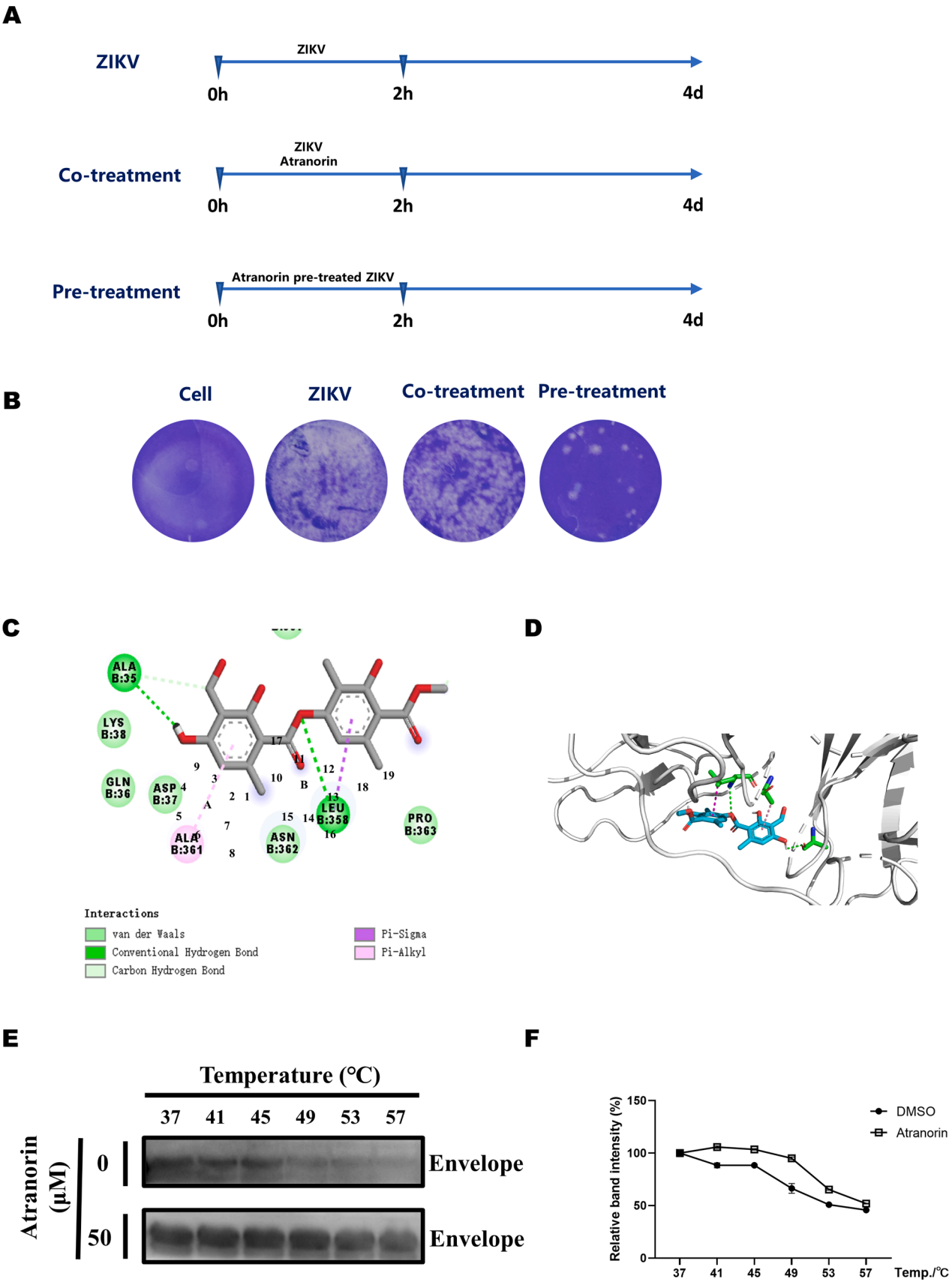

Fig. 7. Atranorin exerted anti-ZIKV activity by targeting viral envelope protein. A. Schematic diagram of virus infectivity assay. B. Plaque assay showing the infectious ability of ZIKV. C, D. The predicted binding pose (C) and interacting residues (D) between atranorin and ZIKV E protein. E, F. The thermal stability of envelope protein in E. coli lysates. The experiments were repeated for three times.

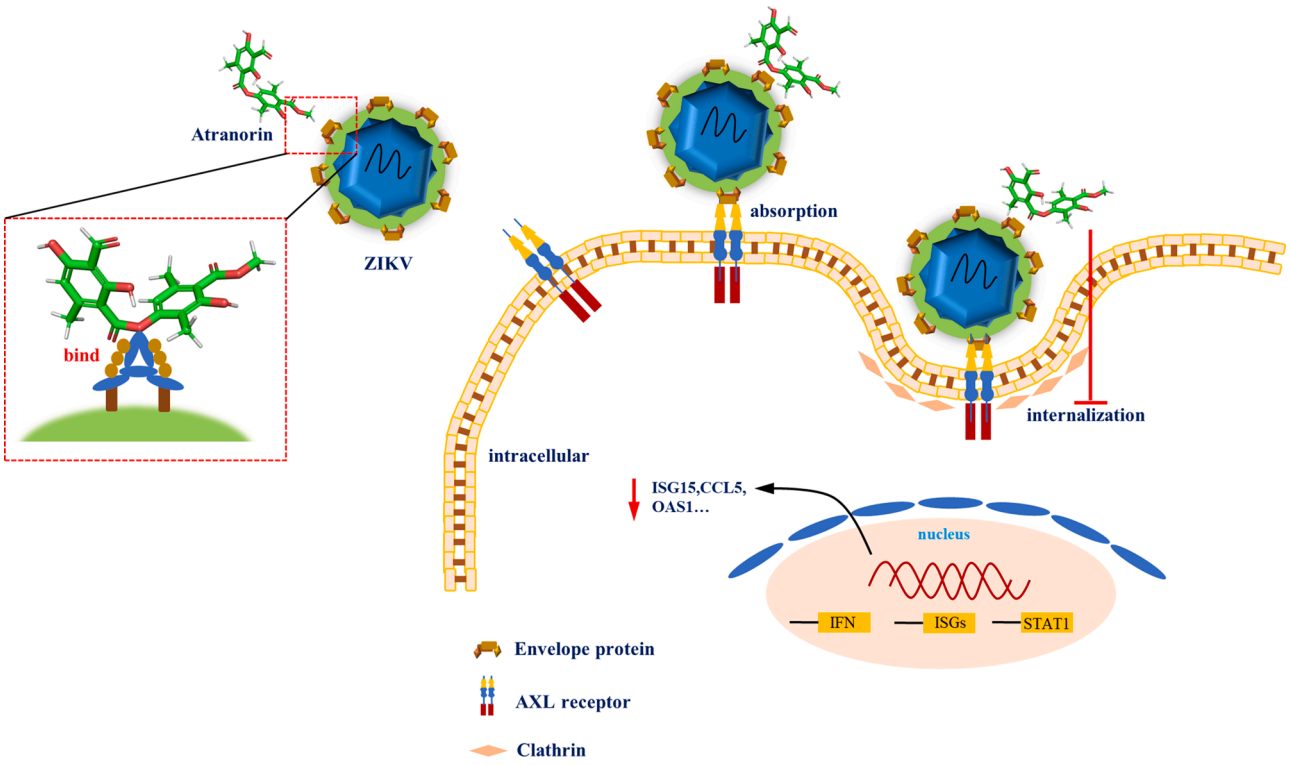

Fig. 8. Atranorin inhibits ZIKV infection in SNB-19 cells *via* targeting ZIKV envelope protein. Atranorin displays anti-ZIKV activity and inhibits ZIKV induced IFN signal pathway activation and innate immune responses in human glioma cell line SNB-19. Mechanistically, atranorin has no influence on AXL-dependent virus adsorption and clathrin-mediated endocytosis. Instead, atranorin directly binds to ZIKV envelop protein, therefore lowering ZIKV infectivity and blocking ZIKV internalization.

protein in mediating ZIKV entry, we speculate that atranorin might directly target ZIKV envelope protein. The ZIKV E monomer is composed of three distinct domains in the ectodomain: central β-barrel domain I (DI), extended finger-dimerization domain II (DII), and immunoglobulin-like domain III (DIII). DI acts as a bridge between DII and DIII. The DI-DII hinge is important for turning over DII to expose the FL during the fusion process (Lin et al., 2018). Molecular docking predicted that atranorin might bind to the domains I and III of E protein. Further, the binding interaction between atranorin and E protein was confirmed by thermal shift assay. Combining the above results, we indicated that atranorin might inhibit the ZIKV entry by targeting the viral envelope protein. Actually, the antiviral role of small molecules by interacting with envelope proteins has also been demonstrated in other studies (Lian et al., 2018; Mangan et al., 2019; Pitts et al., 2019). Recently, some scientists proposed a conserved pocket of envelope protein as a target for developing broad-spectrum antivirals against multiple, mosquito-borne flavivirus pathogens (de Wispelaere et al., 2018). These results instruct us that atranorin might also exert antiviral activity towards other virus that share similar patterns of envelope protein for atranorin binding. The precise binding mode of atranorin towards ZIKV envelope protein and the potential activity of atranorin against other virus would be included in our future study.

Conclusion

We identified atranorin as a potent anti-ZIKV compound on the human glioma cell line SNB-19. Also, we revealed that atranorin inhibits ZIKV infection through binding to viral envelope protein and therefore inhibiting ZIKV entry (Fig. 8). Our research not only provided an experimental basis for the further development of atranorin, but also offered a reference for finding antiviral drugs from natural products.

Funding

This work was supported by the grants of National Key R&D Program of China (No. 2021YFC2300700).

CRediT authorship contribution statement

Guan-gen Huang: Writing – original draft, Visualization, Methodology, Investigation, Formal analysis, Data curation, Conceptualization. **Hao-yu Wang:** Writing – review & editing, Methodology, Investigation, Formal analysis, Data curation, Conceptualization. **Xiao-han Wang:** Methodology, Investigation, Data curation, Conceptualization. **Tao Yang:** Methodology, Investigation, Data curation, Conceptualization. **Xiao-meng Zhang:** Validation, Methodology, Investigation. **Chun-lan Feng:** Supervision, Resources. **Wei-min Zhao:** Resources. **Wei Tang:** Writing – review & editing, Supervision, Resources, Project administration, Methodology, Investigation, Funding acquisition, Conceptualization.

Declaration of competing interest

The authors declare no competing interests.

Acknowledgments

We thank Meng-meng Xu and Jing-Ren for their kind assistance to this study.

Supplementary materials

Supplementary material associated with this article can be found, in the online version, at doi:10.1016/j.phymed.2024.155343.

References

Agrelli, A., de Moura, R.R., Crovella, S., Brandão, L.A.C., 2019. Zika virus entry mechanisms in human cells. Infect. Genet. Evol. 69, 22–29.

Barrows, N.J., Campos, R.K., Liao, K.C., Prasanth, K.R., Soto-Acosta, R., Yeh, S.C., Schott-Lerner, G., Pompon, J., Sessions, O.M., Bradrick, S.S., Garcia-Blanco, M.A., 2018. Biochemistry and molecular biology of flaviviruses. Chem. Rev. 118, 4448–4482.

Clark, M.J., Miduturu, C., Schmidt, A.G., Zhu, X., Pitts, J.D., Wang, J., Potisopon, S., Zhang, J., Wojciechowski, A., Hann Chu, J.J., Gray, N.S., Yang, P.L., 2016. Gnf-2 inhibits dengue virus by targeting ABL kinases and the viral E protein. Cell Chem. Biol. 23, 443–452.

de Wispelaere, M., Lian, W., Potisopon, S., Li, P.C., Jang, J., Ficarro, S.B., Clark, M.J., Zhu, X., Kaplan, J.B., Pitts, J.D., Wales, T.E., Wang, J., Engen, J.R., Marto, J.A., Gray, N.S., Yang, P.L., 2018. Inhibition of flaviviruses by targeting a conserved pocket on the viral envelope protein. Cell Chem. Biol. 25, 1006–1016 e1008.

Ferraris, P., Yssel, H., Missé, D., 2019. Zika virus infection: an update. Microbes Infect. 21, 353–360.

Giraldo, M.I., Gonzalez-Orozco, M., Rajsbaum, R., 2023. Pathogenesis of Zika virus infection. Annu. Rev. Pathol. 18, 181–203.

Hu, Y., Sun, L., 2019. Systematic analysis of structure similarity between zika virus and other flaviviruses. ACS Infect. Dis. 5, 1070–1080.

Ihunwo, A.O., Perego, J., Martino, G., Vicenzi, E., Panina-Bordignon, P., 2022. Neurogenesis and viral infection. Front. Immunol. 13, 826091.

Irie, S., Tavassoli, M., 1987. Transferrin-mediated cellular iron uptake. Am. J. Med. Sci. 293, 103–111.

Kampmann, T., Yennamalli, R., Campbell, P., Stoermer, M.J., Fairlie, D.P., Kobe, B., Young, P.R., 2009. In silico screening of small molecule libraries using the dengue virus envelope e protein has identified compounds with antiviral activity against multiple flaviviruses. Antiviral Res. 84, 234–241.

Laureti, M., Narayanan, D., Rodriguez-Andres, J., Fazakerley, J.K., Kedzierski, L., 2018. Flavivirus receptors: diversity, identity, and cell entry. Front. Immunol. 9, 2180.

Lian, W., Jang, J., Potisopon, S., Li, P.C., Rahmeh, A., Wang, J., Kwiatkowski, N.P., Gray, N.S., Yang, P.L., 2018. Discovery of immunologically inspired small molecules that target the viral envelope protein. ACS Infect. Dis. 4, 1395–1406.

Lin, H.H., Yip, B.S., Huang, L.M., Wu, S.C., 2018. Zika virus structural biology and progress in vaccine development. Biotechnol. Adv. 36, 47–53.

Mangan, R.J., Stamper, L., Ohashi, T., Eudailey, J.A., Go, E.P., Jaeger, F.H., Itell, H.L., Watts, B.E., Fouda, G.G., Erickson, H.P., Alam, S.M., Desaire, H., Permar, S.R., 2019. Determinants of Tenascin-C and HIV-1 envelope binding and neutralization. Mucosal Immunol. 12, 1004–1012.

Owczarek, K., Chykunova, Y., Jassoy, C., Maksym, B., Rajfur, Z., Pyrc, K., 2019. Zika virus: mapping and reprogramming the entry. Cell Commun. Signal. 17, 41.

Pitts, J., Hsia, C.Y., Lian, W., Wang, J., Pfeil, M.P., Kwiatkowski, N., Li, Z., Jang, J., Gray, N.S., Yang, P.L., 2019. Identification of small molecule inhibitors targeting the Zika virus envelope protein. Antiviral Res. 164, 147–153.

Rauch, I., Müller, M., Decker, T., 2013. The regulation of inflammation by interferons and their stats. JAKSTAT 2, e23820.

Rey, F.A., Stiasny, K., Heinz, F.X., 2017. Flavivirus structural heterogeneity: implications for cell entry. Curr. Opin. Virol. 24, 132–139.

Schneider, W.M., Chevillotte, M.D., Rice, C.M., 2014. Interferon-stimulated genes: a complex web of host defenses. Annu. Rev. Immunol. 32, 513–545.

Song, B.H., Yun, S.I., Woolley, M., Lee, Y.M., 2017. Zika virus: history, epidemiology, transmission, and clinical presentation. J. Neuroimmunol. 308, 50–64.

Stephenson, J., Nutma, E., van der Valk, P., Amor, S., 2018. Inflammation in CNS neurodegenerative diseases. Immunology 154, 204–219.

Studzinska-Sroka, E., Galanty, A., Bylka, W., 2017. Atranorin - an interesting lichen secondary metabolite. Mini Rev. Med. Chem. 17, 1633–1645.

Suzuki, M.T., Parrot, D., Berg, G., Grube, M., Tomasi, S., 2016. Lichens as natural sources of biotechnologically relevant bacteria. Appl. Microbiol. Biotechnol. 100, 583–595.

Tan, J., Wu, B., Chen, T., Fan, C., Zhao, J., Xiong, C., Feng, C., Xiao, R., Ding, C., Tang, W., Zhang, A., 2021. Synthesis and pharmacological evaluation of tetrahydro-γ-carboline derivatives as potent anti-inflammatory agents targeting cyclic GMP-AMP synthase. J. Med. Chem. 64, 7667–7690.

Tolomeo, M., Cavalli, A., Cascio, A., 2022. Stat1 and its crucial role in the control of viral infections. Int. J. Mol. Sci. 23, 4095.

Vu, T.H., Le Lamer, A.C., Lalli, C., Boustie, J., Samson, M., Lohézic-Le Dévéhat, F., Le Seyec, J., 2015. Depsides: lichen metabolites active against hepatitis C virus. PLOS One 10, e0120405.

Wang, H.Y., Lin, X., Huang, G.G., Zhou, R., Lei, S.Y., Ren, J., Zhang, K.R., Feng, C.L., Wu, Y.W., Tang, W., 2023. Atranorin inhibits NLRP3 inflammasome activation by targeting asc and protects NLRP3 inflammasome-driven diseases. Acta Pharmacol. Sin. 44, 1687–1700.

Xu, M.M., Wu, B., Huang, G.G., Feng, C.L., Wang, X.H., Wang, H.Y., Wu, Y.W., Tang, W., 2022. Hemin protects against Zika virus infection by disrupting virus-endosome fusion. Antiviral Res. 203, 105347.

Yu, Y., Shen, M., Song, Q., Xie, J., 2018. Biological activities and pharmaceutical applications of polysaccharide from natural resources: a review. Carbohydr. Polym. 183, 91–101.

Yuan, S., Jiang, S.C., Zhang, Z.W., Fu, Y.F., Hu, J., Li, Z.L., 2021. Quantification of cytokine storms during virus infections. Front. Immunol. 12, 659419.